

In-plane magnetic penetration depth λ_{ab} in $\text{Ca}_{2-x}\text{Na}_x\text{CuO}_2\text{Cl}_2$: Role of the apical sitesR. Khasanov,¹ N. D. Zhigadlo,² J. Karpinski,² and H. Keller¹¹*Physik-Institut der Universität Zürich, Winterthurerstrasse 190, CH-8057 Zürich, Switzerland*²*Laboratory for Solid State Physics, ETH Zürich, CH-8093 Zürich, Switzerland*

(Received 27 March 2007; revised manuscript received 7 July 2007; published 7 September 2007)

A study of the in-plane magnetic penetration depth λ_{ab} in a series of the cuprate superconductors $\text{Ca}_{2-x}\text{Na}_x\text{CuO}_2\text{Cl}_2$ (Na-CCOC) with Na content $x \approx 0.11, 0.12, 0.15, 0.18,$ and 0.19 is reported. The zero-temperature values of $\lambda_{ab}(0)$ were obtained by means of the muon-spin rotation technique, as well as from measurements of the intrinsic susceptibility $\chi^{\text{int}}(0)$ by using the procedure developed by Kanigel *et al.* [Phys. Rev. B **71**, 224511 (2005)]. λ_{ab} at $T=0$ K was found to increase with decreasing doping from $\lambda_{ab}(0) = 316(19)$ nm for the $x \approx 0.19$ sample to $\lambda_{ab}(0) = 430(26)$ nm for the $x \approx 0.11$ one. From a comparison of the present Na-CCOC data with those of $\text{Br}_2\text{Sr}_{2-x}\text{La}_x\text{CuO}_{6+\delta}$ and $\text{La}_{2-x}\text{Sr}_x\text{CuO}_4$ cuprate superconductors, it is concluded that substitution of the apical oxygen by chlorine decreases the coupling between the superconducting CuO_2 planes, leading to an enhancement of the two-dimensional properties of Na-CCOC.

DOI: [10.1103/PhysRevB.76.094505](https://doi.org/10.1103/PhysRevB.76.094505)

PACS number(s): 74.72.Jt, 74.25.Op, 74.25.Ha, 76.75.+i

I. INTRODUCTION

The question if the out-of-plane electronic states are essential for high-temperature superconductivity is a matter of debate for a long time. In fact, the idea that in perovskites with their octahedral oxygen environment, the Jahn-Teller effect may lead to an enhanced electron-phonon coupling has guided Bednorz and Müller in their original search for oxide superconductors.¹ Bearing this in mind, one may ask if, in addition to the planar states, the apical states too play a role in the occurrence of high-temperature superconductivity. There is still no clear answer to this question. On the one hand, observation of superconductivity in materials with apical oxygen replaced by halogen atoms (such as F, Cl, Br)²⁻⁴ as well as the absence of an apical oxygen isotope effect on the transition temperature T_c (Ref. 5) and the zero-temperature in-plane magnetic field penetration depth $\lambda_{ab}(0)$ (Ref. 6) suggest that the apical sites do not play a major role. On the other hand, the doubling of T_c (Ref. 7) and the change of the Fermi surface topology from “holelike” to “electronlike”⁸ in epitaxially strained $\text{La}_{2-x}\text{Sr}_x\text{CuO}_4$ films as well as a clear correlation between the transition temperature at optimal doping and the degree of localization of the axial orbitals in the CuO_2 planes⁹ give evidence that apical states are indeed involved in superconductivity. One should also mention that there are compounds where superconductivity has proven to be induced by apical oxygen doping.^{10,11}

In order to elucidate the role of the apical sites, it is important to clarify the origin of similarities and differences between cuprates with oxygen and halogen atoms (such as F, Cl, Br) on the apical sites. Crucial information can be obtained from measurements of the magnetic field penetration depth λ . λ is one of the fundamental lengths of a superconductor which, within a simple London model, relates two important superconducting parameters, the charge carrier concentration n_s and the mass of the charge carriers m^* , according to $\lambda^{-2} \propto n_s/m^*$. The temperature dependence of λ reflects the quasiparticle density of states available for thermal excitations and, therefore, probes the superconducting gap structure. The shape of $\lambda(T)$ and the zero-temperature

value $\lambda(0)$ provides relevant information on the superconducting mechanism and sets a scale for the screening of an external magnetic field. Here, we report studies of the in-plane magnetic penetration depth λ_{ab} for a series of $\text{Ca}_{2-x}\text{Na}_x\text{CuO}_2\text{Cl}_2$ (Na-CCOC) samples with $x \approx 0.11, 0.12, 0.15, 0.18,$ and 0.19 . $\text{Ca}_{2-x}\text{Na}_x\text{CuO}_2\text{Cl}_2$ is a structural analog to the $\text{La}_{2-x}\text{Sr}_x\text{CuO}_4$ with Cl atoms replacing oxygen on the apical sites. The zero-temperature values of λ_{ab} were obtained by means of muon-spin rotation (μSR) as well as from measurements of the intrinsic susceptibility $\chi^{\text{int}}(0)$ by using the procedure developed by Kanigel *et al.*¹² It was found that the measured $\lambda_{ab}(0)$ data points for Na-CCOC are all shifted to the left side of the universal Uemura line, which represents a linear correlation between the zero-temperature superfluid density $\rho_s \propto \lambda_{ab}^{-2}(0)$ and the transition temperature T_c for various hole-doped high-temperature cuprate superconductors (HTS's).^{13,14} Based on a comparison of the Na-CCOC data with the data of $\text{Bi}_2\text{Sr}_{2-x}\text{La}_x\text{CuO}_{6+\delta}$ (Bi2201) and $\text{La}_{2-x}\text{Sr}_x\text{CuO}_4$ (La214), it is concluded that replacing of apical oxygen by Cl decreases the coupling between the superconducting CuO_2 planes, leading to an enhancement of the two-dimensional properties of Na-CCOC. The reason for this is very likely due to a substantial reduction of the amount of holes on the apical sites in comparison to La214. In addition, field-induced magnetism was detected in optimally doped $\text{Ca}_{1.82}\text{Na}_{0.18}\text{CuO}_2\text{Cl}_2$, suggesting that Na-CCOC has a competing magnetic state very close in free energy to their superconducting state.

The paper is organized as follows. In Sec. II we describe the sample preparation procedure and details of the muon-spin rotation and magnetization experiments. The dependence of the muon-spin depolarization rate σ on temperature and magnetic field is presented in Sec. III A. Sections III B and III C comprise studies of the in-plane magnetic penetration depth λ_{ab} by means of μSR and magnetization techniques. The comparison of the superfluid density $\rho_s \propto \lambda_{ab}^{-2}(0)$ for Na-CCOC with that for other hole-doped HTS's with oxygen on the apical site is presented in Sec. IV A. The two-dimensional aspects of the superfluid density are discussed in Sec. IV B. The conclusions follow in Sec. V.

II. EXPERIMENTAL DETAILS

Underdoped and optimally doped superconducting $\text{Ca}_{2-x}\text{Na}_x\text{CuO}_2\text{Cl}_2$ samples with Na content $x \approx 0.11, 0.12, 0.15, 0.18,$ and 0.19 were synthesized under high pressure by using the procedure described in Ref. 15. It includes, first, the synthesis of the nonsuperconducting parent compound $\text{Ca}_2\text{CuO}_2\text{Cl}_2$ and, second, the high-pressure annealing of $\text{Ca}_2\text{CuO}_2\text{Cl}_2$ mixed with NaClO_4 and NaCl . $\text{Ca}_2\text{CuO}_2\text{Cl}_2$ was synthesized by a solid-state reaction of Ca_2CuO_3 , CuO , and CaCl_2 . The powder mixture was pressed into a pellet and synthesized at 750°C in argon flow with several intermediate grindings under ambient pressure. The resulting $\text{Ca}_2\text{CuO}_2\text{Cl}_2$ was well mixed with NaClO_4 and NaCl in a molar ratio of 1:0.2:0.2 in a dry box and sealed in Pt cylindrical capsules of 6–8 mm internal diameter and 7–9 mm length. High-pressure experiments were performed in opposed anvil-type high-pressure devices at 40–45 kbar. After applying pressure, the temperature was increased for 1.5 h up to the maximum of 1350–1700 $^\circ\text{C}$ and kept stable for 0.5 h. Then, the temperature was slowly decreased to 1000 $^\circ\text{C}$ and, finally, to room temperature. The high pressure was maintained constant throughout the synthesis and was removed only after the cell was cooled to room temperature. The Na content was estimated from the comparison of the c -axis lattice constants obtained in x-ray experiments with those reported in Refs. 3 and 16. Due to extreme high hygroscopicity of $\text{Ca}_{2-x}\text{Na}_x\text{CuO}_2\text{Cl}_2$, all the manipulations with the samples were made in the glovebox filled with Ar.

Zero-field and transverse-field μSR experiments were performed at the πM3 and πE1 beam lines at the Paul Scherrer Institute (Villigen, Switzerland). The μSR experiments were performed on two samples: an optimally doped sample with Na content $x \approx 0.18$ ($T_c \approx 27$ K) and a slightly underdoped one with $x \approx 0.12$ ($T_c \approx 18$ K). In a superconducting sample, the magnetic penetration depth λ can be extracted from the second moment $\langle \Delta B^2 \rangle$ of the probability distribution of the local magnetic field $P(B)$ in the mixed state probed by μSR .¹⁷ In the present study, we first analyzed the μSR time spectra by using a direct Fourier transform based on a maximum entropy algorithm,¹⁸ with no prior assumptions on the form of $P(B)$. It was found that a Gaussian distribution of local fields gives a reasonable estimate of $P(B)$ (see Fig. 1), in agreement with previous observations.¹⁹ Therefore, the μSR time spectra were analyzed by using a Gaussian relaxation function $R(t) = \exp[-\sigma^2 t^2 / 2]$. The second moment of $P(B)$ was then obtained as $\langle \Delta B^2 \rangle = \sigma^2 / \gamma_\mu^2$ ($\gamma_\mu = 2\pi \times 135.5342$ MHz/T is the muon gyromagnetic ratio).

The field-cooled 0.5 mT magnetization measurements for the Na-CCOC samples ($x \approx 0.11, 0.12, 0.15, 0.18,$ and 0.19) were performed by using a superconducting quantum interference device magnetometer. In order to follow the procedure described in Ref. 12, the samples used for the magnetization experiments were preliminary powderized and then placed in quartz ampoules (1.5 mm inner diameter). The masses of the samples were ~ 25 – 30 mg. The ratio of the diameter to the height of the powder in the ampoule was approximately 1–7. The magnetic field was applied parallel to the ampoule axis. As shown in Ref. 12, for this geometry

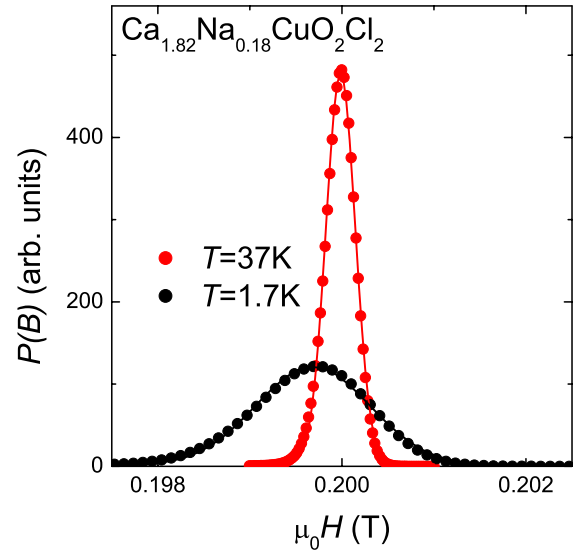


FIG. 1. (Color online) Internal magnetic field distribution $P(B)$ for $\text{Ca}_{1.82}\text{Na}_{0.18}\text{CuO}_2\text{Cl}_2$ sample at $\mu_0 H = 0.2$ T in the normal ($T = 37$ K) and the superconducting ($T = 1.7$ K) state obtained by means of the maximum entropy Fourier transform technique. The solid lines represent fits with a single Gaussian line.

the zero-temperature “intrinsic” susceptibility, obtained from the field-cooled magnetization, is proportional to the inverse squared in-plane magnetic penetration depth, $\chi^{\text{int}}(0) \propto \lambda_{ab}^{-2}(0)$.

III. EXPERIMENTAL RESULTS

A. Dependence of the muon-spin depolarization rate σ on T and H

Figure 2 shows the temperature dependences of the muon-spin depolarization rate σ obtained from the fits to the μSR data. It is seen that for both Na-CCOC samples studied by μSR , $\sigma(T)$ is constant above T_c and starts to rise with decreasing temperature for $T < T_c$. Most interestingly, however, is that in the low-temperature region an inflection point (T_{ip}) appears below which σ starts to increase rather sharply. It is also seen that with increasing magnetic field, σ below T_{ip} rises faster and T_{ip} has a tendency to shift to higher temperatures. Indeed, the inset in Fig. 2(a) shows that when the magnetic field increases from 0.2 to 0.64 T, T_{ip} for the $x \approx 0.18$ sample shifts from approximately 4 to 6 K and the ratio $\sigma(1.7\text{ K}) / \sigma(T_{ip})$ changes from 1.05 to 1.20. The behavior of $\sigma(T)$ below T_{ip} clearly demonstrates that some kind of magnetic ordering takes place in Na-CCOC. The zero-field μSR experiments of Ohishi *et al.*,²⁰ performed on a series of Na-CCOC ($x = 0.0$ – 0.12) samples, reveal the presence of spin-glass-type magnetism in the $x = 0.12$ sample with a spin-glass ordering temperature of ≈ 2.5 K. This suggests that the increase of σ at $T < T_{ip}$, seen in Fig. 2(b), is simply a consequence of it. The situation for the $x \approx 0.18$ sample is, however, not so clear. Our zero-field μSR experiments gave no indication for any magnetism in this particular sample down to $T \approx 1.7$ K. On the other hand, the increase of $\sigma(T)$ below

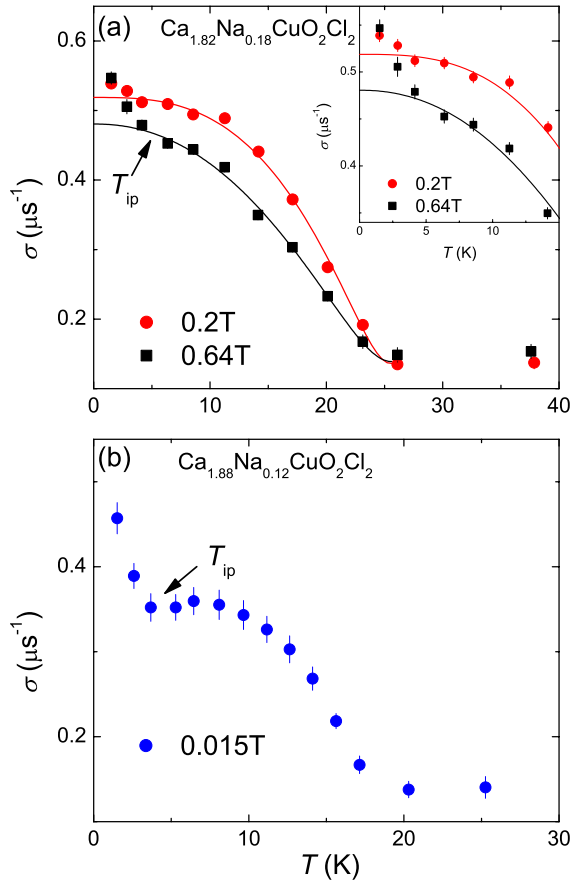


FIG. 2. (Color online) (a) Temperature dependence of the muon-spin depolarization rate σ for $\text{Ca}_{1.82}\text{Na}_{0.18}\text{CuO}_2\text{Cl}_2$ measured after field cooling in $\mu_0 H = 0.2$ T (red circles) and 0.64 T (black squares). (b) $\sigma(T)$ for $\text{Ca}_{1.88}\text{Na}_{0.12}\text{CuO}_2\text{Cl}_2$ measured in $\mu_0 H = 0.015$ T. The solid lines in (a) represent fits of Eq. (2) to the data. See text for details. The inset in (a) shows the extension of the low-temperature region.

T_{ip} and the shift of T_{ip} to higher temperatures, both correlated with the magnetic field [see inset of Fig. 2(a)], clearly demonstrate the appearance and enhancement of magnetism in the $x \approx 0.18$ sample. Note that field-induced magnetism was recently observed by Savici *et al.*²¹ in highly underdoped $\text{La}_{2-x}\text{Sr}_x\text{CuO}_4$, $\text{La}_{2-x}\text{Ba}_x\text{CuO}_4$, and $\text{La}_{2-x}\text{Eu}_x\text{CuO}_4$ HTS's. It was shown that the increase of the relaxation above the antiferromagnetic ordering temperature T_N and the superconducting transition temperature T_c is due to quasistatic random fields induced by the external magnetic field.²¹

In order to study field-induced magnetism in the $x \approx 0.18$ sample in more detail, σ was measured as a function of H above (37 K) and below (1.7 K) the superconducting transition temperature (Fig. 3). Note that all $\sigma(1.7$ K) data points were obtained after field cooling the sample from far above T_c to 1.7 K in the corresponding field. Above T_c , the magnetic contribution σ_m was obtained by subtracting the nuclear contribution ($\sigma_{nm} = 0.132 \mu\text{s}^{-1}$ at $\mu_0 H = 0.01$ T) from the measured σ as $\sigma_m^2 = \sigma^2 - \sigma_{nm}^2$. In order to obtain σ_m at $T = 1.7$ K, we used the following procedure. Bearing in mind that below T_c a superconducting component σ_{sc} is present, the total σ obtained in μSR experiments is a sum of²²

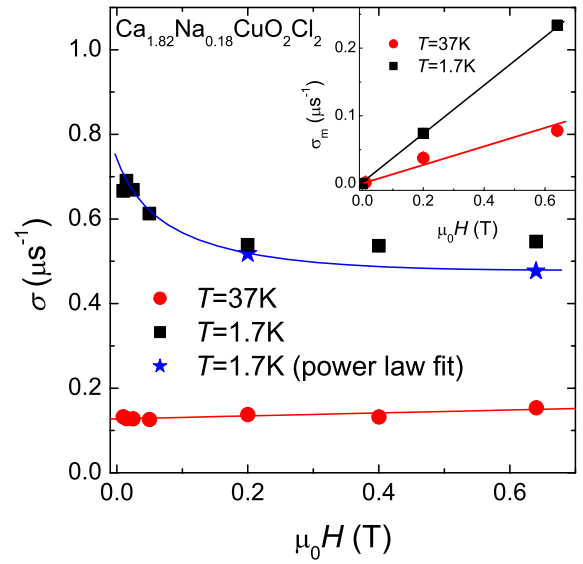


FIG. 3. (Color online) Magnetic field dependence of the muon-spin depolarization rate of $\text{Ca}_{1.82}\text{Na}_{0.18}\text{CuO}_2\text{Cl}_2$ above (red circles) and below (black squares) the superconducting transition temperature. Stars are the $\sigma(T = 1.7$ K) values obtained after subtraction of the magnetic contribution σ_m . The blue and the red lines are guides for the eye. The inset shows $\sigma_m(H)$ at $T = 37$ K (red circles) and $T = 1.7$ K (black squares). See text for details.

$$\sigma^2(T) = \sigma_m^2(T) + \sigma_{sc}^2(T) + \sigma_{nm}^2(T). \quad (1)$$

In the next step, we assumed that σ_{nm} does not depend on temperature and that in the temperature range $T_{ip} < T < T_c$ the measured $\sigma(T)$ is determined predominantly by the superconducting part of the muon-spin depolarization rate $\sigma_{sc}(T)$ and the nuclear dipolar component σ_{nm} . The temperature dependence of $\sigma_{sc}(T)$ was assumed to be described by the power law¹⁷

$$\sigma_{sc}(T) = \sigma_{sc}(0)[1 - (T/T_c)^n]. \quad (2)$$

The corresponding fitting curves are shown in Fig. 2(a). Finally, σ_m at $T = 1.7$ K was calculated as $\sigma_m(1.7$ K) $= [\sigma^2(1.7$ K) $- \sigma_{sc}^2(1.7$ K) $- \sigma_{nm}^2]^{0.5}$. The field dependence of σ_m for $T = 1.7$ and 37 K is shown in the inset of Fig. 3. It is seen that for both temperatures, σ_m increases linearly with increasing magnetic field, in good agreement with the results of Savici *et al.*²¹ We want to point, however, to the difference between the optimally doped $\text{Ca}_{1.82}\text{Na}_{0.18}\text{CuO}_2\text{Cl}_2$ sample measured here and the underdoped $\text{La}_{2-x}\text{Sr}_x\text{CuO}_4$, $\text{La}_{2-x}\text{Ba}_x\text{CuO}_4$, and $\text{La}_{2-x}\text{Eu}_x\text{CuO}_4$ HTS's studied in Ref. 21. Until now, field-induced magnetism was observed only for systems exhibiting static magnetism in zero field.²¹ This is not the case for the $x \approx 0.18$ sample, since no magnetism was detected in zero-field μSR experiments down to ≈ 1.7 K. Even though we cannot rule out completely the appearance of zero-field magnetism at lower temperatures, the enhancement of magnetism with increasing field would imply that optimally doped Na-CCOC has a competing magnetic state very close in free energy to their superconducting state.

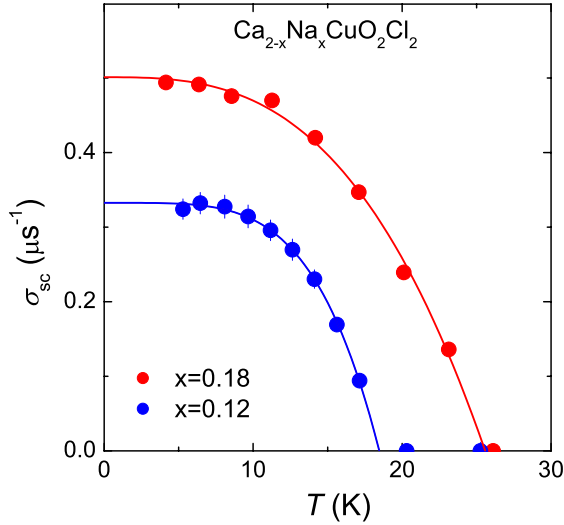


FIG. 4. (Color online) Temperature dependences of $\sigma_{sc} \propto \lambda_{ab}^{-2}$ for $\text{Ca}_{2-x}\text{Na}_x\text{CuO}_2\text{Cl}_2$ ($x \approx 0.18$, upper curve; $x \approx 0.12$, lower curve). The solid lines represent power law fits to the data. See text for details.

B. Determination of $\lambda_{ab}(0)$ by means of muon-spin rotation

In earlier transverse-field μSR experiments on $\text{YBa}_2\text{Cu}_3\text{O}_{7-\delta}$, it was observed that the relaxation rate σ for nonoriented powders exhibits nearly no magnetic field dependence in a rather broad field range (typically, from ~ 0.05 to ~ 0.4 T).¹⁷ This can be explained within the London model which predicts that the second moment of the magnetic field distribution in a perfect vortex lattice is independent of the applied magnetic field for $2H_{c1} \leq H \ll H_{c2}$ (H_{c1} and H_{c2} are the first and the second critical fields, respectively).²³ This feature allows a direct comparison of values of σ_{sc} obtained for various HTS's at various doping levels and taken at different magnetic fields. In order to check if the relation $\sigma_{sc}(H) \approx \text{const}$ also holds for Na-CCOC, we subtract the magnetic contribution σ_m for $\mu_0 H = 0.2$ and 0.64 T from the measured σ in accordance with Eq. (1) and plot the resulting $(\sigma_{sc}^2 + \sigma_{nm}^2)^{0.5}$ values (blue stars) in Fig. 3. Two tendencies are clearly seen: First, for fields smaller than 0.2 T, one can almost neglect the magnetic contribution σ_m to the measured σ . This is confirmed by the field dependence of σ_m presented in the inset of Fig. 3, revealing that for $\mu_0 H < 0.2$ T the σ_m at $T = 1.7$ K is more than five times smaller than the measured σ . Second, the solid blue line shows that for the $x \approx 0.18$ sample, the relation $\sigma_{sc}(H) \approx \text{const}$ holds for $\mu_0 H \geq 0.15$ T. The slow decrease of σ_{sc} above 0.15 T can be explained by nonlocal and nonlinear corrections to σ_{sc} due to the d -wave order parameter of HTS.^{24–26}

Figure 4 shows the temperature dependence of σ_{sc} , obtained after subtraction of σ_{nm} from the data presented in Fig. 2. Since at low temperatures a magnetic contribution is present, data points below 4 K were excluded in the analysis. The solid lines represent fits to the power law [Eq. (2)]. From the obtained values of $\sigma_{sc}(0)$, the zero-temperature values of

TABLE I. Summary of the $\lambda(T)$ study of $\text{Ca}_{2-x}\text{Na}_x\text{CuO}_2\text{Cl}_2$ (see text for details).

Method	x	T_c (K)	$\sigma_{sc}(0)$ (μs^{-1})	$\chi^{int}(0)$	$\lambda_{ab}(0)$ (nm)
μSR	0.12	18.5(2)	0.33(2)		390(24)
	0.18	25.6(2)	0.50(3)		317(19)
$\chi^{int}(0)$	0.11	15.14(4)		0.171	430(26)
	0.12	18.40(3)		0.192	406(24)
	0.15	23.45(3)		0.307	321(19)
	0.18	27.11(3)		0.315	317(19) ^a
	0.19	27.70(3)		0.316	316(19)

^aNormalized to $\lambda_{ab}(0) = 317(19)$ nm obtained for the $x \approx 0.18$ sample in μSR experiment.

the in-plane magnetic field penetration depth $\lambda_{ab}(0)$ were determined as¹⁷

$$\lambda_{ab}(\text{nm}) = \frac{224}{\sqrt{\sigma_{sc}(\mu\text{s}^{-1})}}. \quad (3)$$

The results of the fits and the values of $\lambda_{ab}(0)$ obtained by Eq. (3) are summarized in Table I. Note that $\lambda_{ab}(0) = 317(19)$ nm for $x \approx 0.18$ sample is more than 40% smaller than $\lambda_{ab}(0) = 438\text{--}453$ nm reported by Kim *et al.*²⁷ This is probably due to the fact that $\lambda_{ab}(0)$ in Ref. 27 was obtained indirectly from the fit of reversible magnetization data by means of Hao-Clem model in a rather tight temperature region, namely, from 14.5 to 20 K only. In the present study, λ_{ab} was directly derived by μSR in a broad range of temperatures (from T_c down to 4 K) and, we think, it is more reliable.

C. Determination of $\lambda_{ab}(0)$ in low-field magnetization experiments

In order to complete the in-plane magnetic field penetration depth study of the HTS Na-CCOC, we performed similar field-cooled magnetization (M_{FC}) experiments as reported by Kanigel *et al.*¹² It was shown that for HTS powder samples, shaped in a cylindrical container having a diameter much smaller than its length, $\lambda_{ab}(0)$ can be obtained from the so-called intrinsic susceptibility $\chi^{int}(0) = M_{FC}(0)/M_{id}$ (M_{id} is the magnetization of an ideal diamagnet) according to the relation $\chi^{int}(0) \propto \lambda_{ab}^{-2}(0)$.¹² Figure 5 shows $M_{FC}(T)$ curves for $\text{Ca}_{2-x}\text{Na}_x\text{CuO}_2\text{Cl}_2$ ($x \approx 0.11, 0.12, 0.15, 0.18,$ and 0.19) samples taken at 0.5 mT. The transition temperatures T_c and the values of $\chi^{int}(0)$ were obtained from the intersection of the linearly extrapolated M_{FC} curves with the $M = 0$ line and by extrapolating the low-temperature part of $M_{FC}(T)$ to $T = 0$, respectively (see Fig. 5 and Table I). From the measured values of $\chi^{int}(0)$, the zero-temperature values of $\lambda_{ab}(0)$ were then obtained by normalizing to $\lambda_{ab}(0) = 317(19)$ nm derived for the $\text{Ca}_{1.82}\text{Na}_{0.18}\text{CuO}_2\text{Cl}_2$ sample by μSR (see Table I). A quick glance at Table I reveals that the procedure described

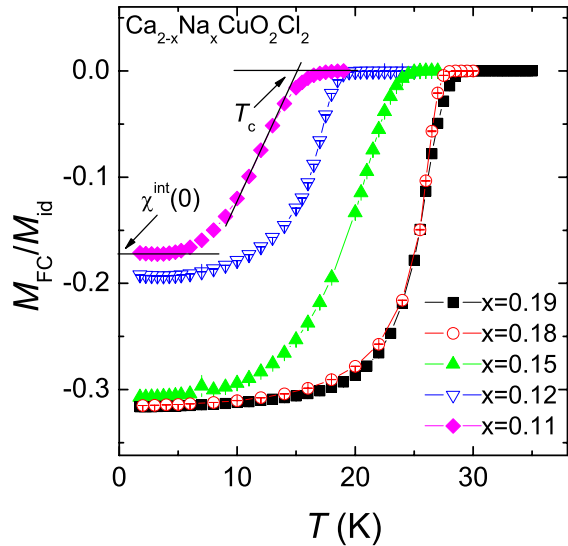


FIG. 5. (Color online) Temperature dependence of the field-cooled magnetization M_{FC} ($\mu_0 H = 0.5$ mT) normalized to magnetization of an ideal diamagnet M_{id} for $\text{Ca}_{2-x}\text{Na}_x\text{CuO}_2\text{Cl}_2$. From the left to the right, $x \approx 0.11, 0.12, 0.15, 0.18$, and 0.19 .

in Ref. 12 is indeed reliable, since the values of $\lambda_{ab}(0)$ for the $x \approx 0.12$ sample obtained by means of both techniques used in the present study agree rather well.

IV. DISCUSSIONS

A. Comparison with superfluid densities of high-temperature superconductors with oxygen on the apical site

To compare the results for Na-CCOC with the results for other hole-doped superconductors, in Fig. 6 we plot T_c as a function of the zero-temperature superfluid density $\rho_s \propto \lambda^{-2}(0) \propto \sigma_{sc}(0)$. We also include data points for Na-CCOC ($x=0.18$),²⁷ for the structurally related compound with oxygen on the apical site La214,^{14,28} for the single-layer HTS Bi2201,²⁹ and for underdoped $\text{YBa}_2\text{Cu}_3\text{O}_{7-\delta}$ (Y123) with highly reduced T_c .³⁰ The dashed line represents the famous “Uemura” relation [linear correlation between T_c and $\lambda^{-2}(0) \propto n_s/m^*$ for various families of underdoped HTS’s^{13,14}]. It is seen that points for Na-CCOC at all levels of doping as well as points for Bi2201 and highly underdoped Y123 lie significantly higher than expected for the “Uemura” relation. The solid line corresponds to the power law $\sigma_{sc}(0) \propto T_c^{1.6}$ obtained in Ref. 30. While the agreement between Na-CCOC, Bi2201, and highly underdoped Y123 is rather good, the points for the structurally related compound La214 are shifted to the right. Only 4 out of 18 points coincide with those for Na-CCOC: three points for underdoped La214 with highly reduced T_c ’s and one for overdoped La214 ($T_c \approx 32$ K). As was recently pointed out by Russo *et al.*,²⁹ the agreement with underdoped Y123 and with points for underdoped La214 should be taken with caution. It was shown by zero-field μSR experiments on La214 (Ref. 31) and Y123 (Ref. 32) having rather reduced T_c ’s that a major volume fraction exhibits static magnetic order and, probably, does not carry the

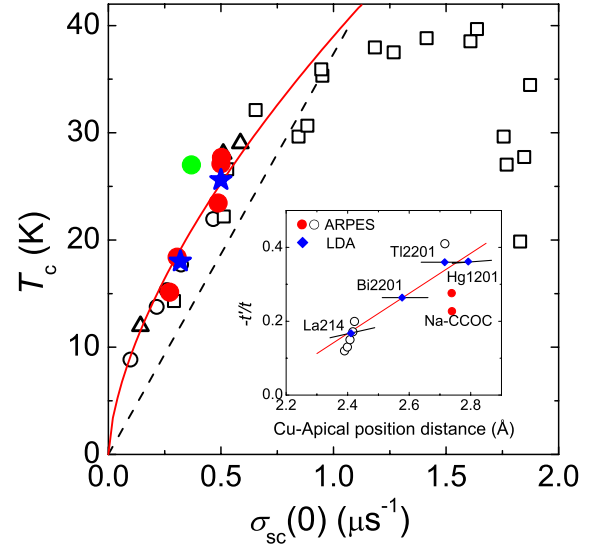


FIG. 6. (Color online) T_c vs $\sigma_{sc}(0) \propto \lambda_{ab}^{-2}$ for Na-CCOC and various hole-doped HTS’s with oxygen on the apical site. Solid red circles and blue stars are Na-CCOC data obtained in the present study (see Table I). The green circle is the data point for Na-CCOC ($x=0.18$) from Ref. 27. Open squares are La214 data from Refs. 14 and 28. Open triangles are Bi2201 data taken from Ref. 29 and open circles are Y123 data from Ref. 30. The dashed line represents the “Uemura” relation (Refs. 13 and 14). The solid red line corresponds to the power law with $\sigma_{sc}(0) \propto T_c^{1.6}$ from Ref. 30. The inset shows the hopping integral ratio t'/t as a function of plane Cu -apical position distance for La214, Bi2201, Tl2201, and Hg2201 HTS’s obtained from local-density approximation (LDA) band structure calculations (after Ref. 9). The circles are t'/t values for Na-CCOC ($x=0.10, 0.12$) (Ref. 36), La214 (Ref. 37), and Tl2201 (Ref. 38) obtained from ARPES data. See text for details.

superfluid.³³ Thus, the reduction of the superfluid density for both of these compounds may be a simple consequence of it.²⁹ In contrast, the results for Bi2201 were obtained for samples which do not involve static magnetic order²⁹ and, correspondingly, might represent an intrinsic property free of possible complications due to magnetic fractions. Therefore, we are first going to compare the present Na-CCOC data with those of Bi2201 and, later on, with La214.

The good agreement between the Na-CCOC and Bi2201 data presented in Fig. 6 suggests that there are some similarities between these two compounds: (i) Both Na-CCOC and Bi2201 are highly anisotropic superconductors. Highly two-dimensional (2D) properties of the Na-CCOC system were recently reported by Kim *et al.*²⁷ They found that the fluctuation induced magnetization and the irreversibility line obtained for Na-CCOC ($x=0.18$) show pronounced 2D behavior. The anisotropy coefficient γ was estimated to be in the range $50 < \gamma < 800$. Even though the range of γ reported in Ref. 27 is rather broad, the value of γ is much higher than, e.g., $\gamma=15$ obtained for optimally doped La214,³⁴ but is consistent with $\gamma=400$ for optimally doped Bi2201.³⁵ (ii) The inset in Fig. 6 reveals that both Na-CCOC and Bi2201 have similar values for the hopping integral ratio t'/t (t and t' are the first and the second nearest neighbor transfer integrals between the Cu sites in CuO_2 planes). Pavarini *et al.*⁹

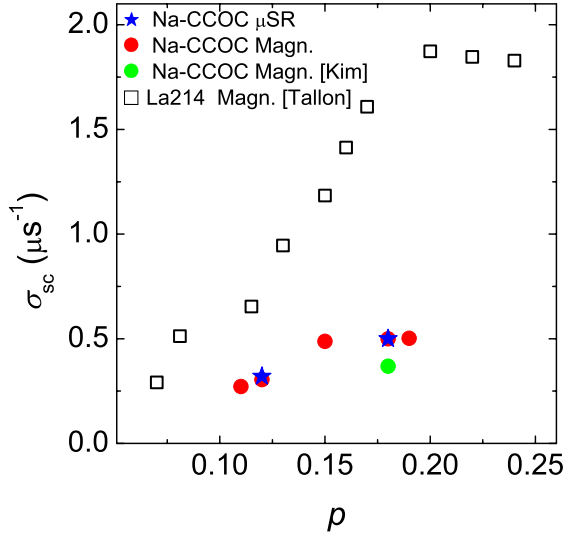


FIG. 7. (Color online) $\sigma_{sc}(0) \propto \lambda_{ab}^{-2}$ vs p (p is the number of holes per planar Cu) for Na-CCOC studied in the present work (solid red circles and blue stars), $x=0.18$ Na-CCOC from Kim *et al.* (Ref. 27) (green circle), and La214 from Tallon *et al.* (Ref. 28) (open squares).

showed that the ratio t'/t is the essential material-dependent parameter which is mainly controlled by the energy of the apical orbital. It was also shown that for hole-doped HTS's, the maximum transition temperature for a particular superconducting family increases with increasing t'/t . In the inset of Fig. 6, we reproduce the original figure from Ref. 9, where t'/t obtained from local-density approximation (LDA) band structure calculations is plotted as a function of the plane Cu apical position distance for the single-layer HTS's La214, Bi2201, Tl2201, and Hg2201. In this figure, we also include the values of t'/t for Na-CCOC ($x=0.10, 0.12$),³⁶ La214,³⁷ and Tl2201 (Ref. 38) obtained from the analysis of angle resolved photoemission (ARPES) data. It is seen that the t'/t ratio for Na-CCOC is very close to that of Bi2201.

In the next step, we compare the Na-CCOC data with those for the structurally related compound La214. The general difference between them is that Cl atoms, instead of oxygen atoms, occupy the apical positions in Na-CCOC. In Fig. 7, we show the dependence of the zero-temperature superfluid density $\rho_s \propto \lambda^{-2}(0) \propto \sigma_{sc}(0)$ as a function of p (p is the number of holes per planar Cu) for Na-CCOC samples studied in the present work and La214 from Ref. 28. For clarity, we also add point for $x=0.18$ Na-CCOC single crystal sample studied by Kim *et al.*²⁷ Note that for both Na-CCOC and La214, p is just the magnitude of x . A comparison of the superfluid density ρ_s of La214 and Na-CCOC at the same level of doping reveals that in the latter one, ρ_s is reduced by more than a factor of 2. Note that a pronounced difference between the superfluid density of optimally doped La214 and Na-CCOC was also mentioned by Kim *et al.*²⁷ They conclude that the reduction of ρ_s in Na-CCOC is due to a decrease of the charge carrier concentration n_s . We suggest the following reason for a possible decrease of n_s : The phase diagram of cuprates is usually interpreted in terms of holes doped into the planar $\text{Cu}_d x_2 y_2 - \text{O} p_\alpha$ ($\alpha=x, y$) antibonding

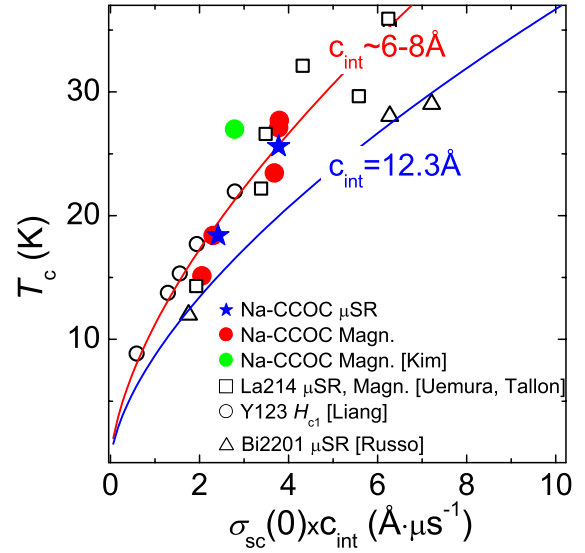


FIG. 8. (Color online) Dependence of the transition temperature T_c on the 2D superfluid density $n_{s2D}/m^* = \sigma_{sc}(0)c_{int}$ for Na-CCOC and various hole-doped HTS's with oxygen on the apical site. Solid red circles and blue stars are Na-CCOC data obtained in the present study. The green circle is the data point for Na-CCOC ($x=0.18$) from Ref. 27. Open squares are La214 data from Refs. 14 and 28. Open triangles are Bi2201 data taken from Ref. 29 and open circles are Y123 data from Ref. 30. The solid lines correspond to the power law with $\sigma_{sc}(0)c_{int} \propto T_c^{1.6}$.

band. In $\text{La}_{2-x}\text{Sr}_x\text{CuO}_4$, it is assumed that one hole per Sr atom enters this band. However, recent *ab initio* calculations yielded additional features appearing on doping of $\text{La}_{2-x}\text{Sr}_x\text{CuO}_4$.³⁹ According to these calculations, part of the holes occupy the $\text{Cu}_d 3z^2 - r^2 - \text{O} p_z$ orbitals. Experimentally, the existence of O 2p holes on the p_z orbitals of the apical oxygen was observed for La214 by polarization-dependent fluorescence yield absorption measurements⁴⁰ and further supported by neutron diffraction studies.⁴¹ In addition, two superconducting condensates with d - and s -wave symmetries were recently observed in slightly overdoped $\text{La}_{1.83}\text{Sr}_{0.17}\text{CuO}_4$.⁴² It was suggested that the s -wave contribution to the total superfluid density arises from the out-of-plane band related with the $\text{Cu}_d 3z^2 - r^2 - \text{O} p_z$ orbitals.⁴² Bearing in mind that for each particular HTS family the transition temperature T_c is determined by the number of holes in the CuO_2 planes, the smaller superfluid density in Na-CCOC in comparison with that in La214 can naturally be explained by a substantial difference in the amount of apical holes in these compounds.

B. The Two-dimensional superfluid density of $\text{Ca}_{2-x}\text{Na}_x\text{CuO}_2\text{Cl}_2$

In order to check further the 2D nature of Na-CCOC, we plot in Fig. 8 the transition temperature T_c as a function of the 2D superfluid density, obtained as $n_{s2D}/m^* = \sigma_{sc}(0)c_{int}$ for the same HTS's as presented in Fig. 6 [c_{int} is the distance between the superconducting CuO_2 planes: $c_{int} = 7.56 \text{ \AA}$ for Na-CCOC,¹⁵ 12.3 \AA for Bi2201,²⁹ and $\approx 6-7 \text{ \AA}$ for Y123

and La214 (Ref. 29)]. As pointed out in Refs. 29 and 43, HTS's with a smaller c_{int} tend to have smaller n_{s2D}/m^* for a given T_c . Recalling the close similarities between Na-CCOC and Bi2201, one expects that data points for these two systems would exhibit the same trend (similar to what is observed in Fig. 6) so that the same n_{s2D}/m^* for Na-CCOC and Bi2201 would correspond to similar values of transition temperatures. It is seen, however, that the data points for Na-CCOC, Y123, and La214 (except the data points for optimally doped and overdoped La214 that are not shown) almost follow the same curve, while those for Bi2201 exhibit a higher 2D superfluid density. This implies that for the same values of n_{s2D}/m^* , the transition temperature in Na-CCOC is expected to be much higher than the corresponding T_c in Bi2201 samples. However, as is seen in Fig. 6, for both Na-CCOC and Bi2201 T_c 's are almost the same. Thus, the substitution of Cl on the apical site leads not only to a pronounced 2D-like behavior due to a reduction of the coupling between the superconducting CuO_2 planes but also to a decrease of the transition temperature T_c . This statement was indeed confirmed in recent theoretical calculation of Yin and Ku.⁴⁴ They showed, in particular, that due to much larger value of $-t'/t$, T_c^{max} is expected to be higher in Na-CCOC than in La214. This is, however, completely opposite to the experimental observations revealing $T_c^{max}=28$ K in Na-CCOC vs $T_c^{max}=38$ K in La214.

V. CONCLUSIONS

$\text{Ca}_{2-x}\text{Na}_x\text{CuO}_2\text{Cl}_2$ is a structural analog to the $\text{La}_{2-x}\text{Sr}_x\text{CuO}_4$ superconductor with Cl atoms replacing oxygen on the apical sites. In order to check the role of the apical oxygen for high-temperature superconductivity, we performed μSR and magnetization studies of the in-plane magnetic penetration depth λ_{ab} for $\text{Ca}_{2-x}\text{Na}_x\text{CuO}_2\text{Cl}_2$ samples with $x \approx 0.11, 0.12, 0.15, 0.18, \text{ and } 0.19$. The following re-

sults were obtained: The absolute value of the in-plane magnetic penetration depth at $T=0$ was found to increase with decreasing doping from $\lambda_{ab}(0)=316(19)$ nm for the $x \approx 0.19$ sample to $\lambda_{ab}(0)=430(26)$ nm for the $x \approx 0.11$ one. Comparison of the superfluid density $\rho_s \propto \lambda_{ab}^{-2}(0) \propto \sigma_{sc}(0)$ of Na-CCOC with that for the structurally related La214 compound reveals that for the same doping level, ρ_s in Na-CCOC is more than a factor of 2 smaller than in La214. The reason for this is very likely due to a substantial decrease of the amount of holes on the apical sites in Na-CCOC. Based on a comparison of the three-dimensional $[\rho_s \propto \sigma_{sc}(0)]$ and the two-dimensional $[n_{s2D}/m^* = \sigma_{sc}(0)c_{int}]$ superfluid density of Na-CCOC with that of Bi2201, it is concluded that replacing apical oxygen by chlorine, first, decreases the coupling between the superconducting CuO_2 planes and, second, leads to a substantial reduction of the transition temperature T_c . In addition, the appearance and enhancement of magnetism with increasing magnetic field was observed for the optimally doped $\text{Ca}_{1.82}\text{Na}_{0.18}\text{CuO}_2\text{Cl}_2$ sample, suggesting that even optimally doped Na-CCOC has a competing magnetic state very close in free energy to its superconducting state. In conclusion, substitution of apical oxygen by chlorine strongly affects the superconducting and the magnetic properties of the cuprate superconductor $\text{Ca}_{2-x}\text{Na}_x\text{CuO}_2\text{Cl}_2$.

ACKNOWLEDGMENTS

This work was partly performed at the Swiss Muon Source ($S\mu S$), Paul Scherrer Institute (PSI, Switzerland). The authors are grateful to A. Amato and R. Scheuermann for assistance during the μSR measurements and S. Weyeneth for helping to prepare the paper. R.K. thanks M. Ermin, Wei Ku, and Wei-Guo Yin for helpful discussions. This work was supported by the Swiss National Science Foundation, the K. Alex Müller Foundation, and in part by the NCCR program MaNEP.

- ¹J. G. Bednorz and K. A. Müller, Z. Phys. B: Condens. Matter **64**, 189 (1986).
- ²M. Al-Mamouri, P. P. Edwards, C. Greaves, and M. Slaski, Nature (London) **369**, 382 (1994).
- ³Z. Hiroi, N. Kobayashi, and M. Takano, Nature (London) **371**, 139 (1994); Physica C **266**, 191 (1996).
- ⁴Y. Zenitani, T. Suzuki, H. Kawashima, and J. Akimitsu, Physica C **419**, 32 (2005).
- ⁵D. Zech, H. Keller, K. Conder, E. Kaldis, E. Liarokapis, N. Poulakakis, and K. A. Müller, Nature (London) **371**, 681 (1994).
- ⁶R. Khasanov, A. Shengelaya, E. Morenzoni, M. Angst, K. Conder, I. M. Savić, D. Lampakis, E. Liarokapis, A. Tassi, and H. Keller, Phys. Rev. B **68**, 220506(R) (2003).
- ⁷J.-P. Locquet, J. Perret, J. Fompeyrine, E. Mächler, J. W. Seo, and G. Van Tendeloo, Nature (London) **394**, 453 (1998).
- ⁸M. Abrecht, D. Ariosa, D. Clotta, S. Mitrovic, M. Onellion, X. X. Xi, G. Margaritondo, and D. Pavuna, Phys. Rev. Lett. **91**, 057002 (2003).
- ⁹E. Pavarini, I. Dasgupta, T. Saha-Dasgupta, O. Jepsen, and O. K.

Andersen, Phys. Rev. Lett. **87**, 047003 (2001).

- ¹⁰C.-Q. Jin, X.-J. Wu, P. Laffez, T. Tatsuki, T. Tamura, S. Adachi, H. Yamauchi, N. Koshizuka, and S. Tanaka, Nature (London) **375**, 301 (1995).
- ¹¹H. Yang, Q. Q. Liu, F. Y. Li, C. Q. Jin, and R. C. Yu, Physica C **453**, 80 (2007).
- ¹²A. Kanigel, A. Keren, A. Knizhnik, and O. Shafir, Phys. Rev. B **71**, 224511 (2005).
- ¹³Y. J. Uemura, G. M. Luke, B. J. Sternlieb, J. H. Brewer, J. F. Carolan, W. N. Hardy, R. Kadono, J. R. Kempton, R. F. Kiefl, S. R. Kreitzman, P. Mulhern, T. M. Riseman, D. Li. Williams, B. X. Yang, S. Uchida, H. Takagi, J. Gopalakrishnan, A. W. Sleight, M. A. Subramanian, C. L. Chien, M. Z. Cieplak, Gang Xiao, V. Y. Lee, B. W. Statt, C. E. Stronach, W. J. Kossler, and X. H. Yu, Phys. Rev. Lett. **62**, 2317 (1989).
- ¹⁴Y. J. Uemura, L. P. Le, G. M. Luke, B. J. Sternlieb, W. D. Wu, J. H. Brewer, T. M. Riseman, C. L. Seaman, M. B. Maple, M. Ishikawa, D. G. Hinks, J. D. Jorgensen, G. Saito, and H. Yamochi, Phys. Rev. Lett. **66**, 2665 (1991).

- ¹⁵N. D. Zhigadlo and J. Karpinski, *Physica C* **460-462**, 372 (2007).
- ¹⁶Y. Kohsaka, M. Azuma, I. Yamada, T. Sasagawa, T. Hanaguri, M. Takano, and H. Takagi, *J. Am. Chem. Soc.* **124**, 12275 (2002).
- ¹⁷P. Zimmermann, H. Keller, S. L. Lee, I. M. Savić, M. Warden, D. Zech, R. Cubitt, E. M. Forgan, E. Kaldis, J. Karpinski, and C. Krüger, *Phys. Rev. B* **52**, 541 (1995).
- ¹⁸B. D. Rainford and G. J. Daniell, *Hyperfine Interact.* **87**, 1129 (1994).
- ¹⁹B. Pümpin, H. Keller, W. Kündig, W. Odermatt, I. M. Savić, J. W. Schneider, H. Simmler, P. Zimmermann, E. Kaldis, S. Rusiecki, Y. Maeno, and C. Rössel, *Phys. Rev. B* **42**, 8019 (1990).
- ²⁰K. Ohishi, I. Yamada, A. Koda, W. Higemoto, S. R. Saha, R. Kadono, K. M. Kojima, M. Azuma, and M. Takano, *J. Phys. Soc. Jpn.* **74**, 2408 (2005).
- ²¹A. T. Savici, A. Fukaya, I. M. Gat-Malureanu, T. Ito, P. L. Russo, Y. J. Uemura, C. R. Wiebe, P. P. Kyriakou, G. J. MacDougall, M. T. Rovers, G. M. Luke, K. M. Kojima, M. Goto, S. Uchida, R. Kadono, K. Yamada, S. Tajima, T. Masui, H. Eisaki, N. Kaneko, M. Greven, and G. D. Gu, *Phys. Rev. Lett.* **95**, 157001 (2005).
- ²²Equation (1) is simply a consequence of the fact that the second moment of the line, consisting of n Gaussian lines, having second moments σ_i^2 and the same first moments, is $\sigma^2 = \sum \sigma_i^2$.
- ²³V. I. Fesenko, V. N. Gorbunov, and V. P. Smilga, *Physica C* **176**, 551 (1991).
- ²⁴J. E. Sonier, J. H. Brewer, and R. F. Kiefl, *Rev. Mod. Phys.* **72**, 769 (2000).
- ²⁵M. H. S. Amin, M. Franz, and I. Affleck, *Phys. Rev. Lett.* **84**, 5864 (2000).
- ²⁶R. Khasanov, A. Shengelaya, D. Di Castro, D. G. Eshchenko, I. M. Savić, K. Conder, E. Pomjakushina, J. Karpinski, S. Kazakov, and H. Keller, *Phys. Rev. B* **75**, 060505(R) (2007).
- ²⁷K.-H. Kim, H.-J. Kim, J.-D. Kim, H.-G. Lee, and S.-I. Lee, *Phys. Rev. B* **72**, 224510 (2005); K.-H. Kim, H.-J. Kim, J.-D. Kim, and H.-G. Lee, *J. Korean Phys. Soc.* **48**, 1032 (2006).
- ²⁸J. L. Tallon, J. W. Loram, J. R. Cooper, C. Panagopoulos, and C. Bernhard, *Phys. Rev. B* **68**, 180501(R) (2003).
- ²⁹P. L. Russo, C. R. Wiebe, Y. J. Uemura, A. T. Savici, G. J. MacDougall, J. Rodriguez, G. M. Luke, N. Kaneko, H. Eisaki, M. Greven, O. P. Vajk, S. Ono, Yoichi Ando, K. Fujita, K. M. Kojima, and S. Uchida, *Phys. Rev. B* **75**, 054511 (2007).
- ³⁰R. Liang, D. A. Bonn, W. N. Hardy, and D. Broun, *Phys. Rev. Lett.* **94**, 117001 (2005).
- ³¹A. T. Savici, Y. Fudamoto, I. M. Gat, T. Ito, M. I. Larkin, Y. J. Uemura, G. M. Luke, K. M. Kojima, Y. S. Lee, M. A. Kastner, R. J. Birgeneau, and K. Yamada, *Phys. Rev. B* **66**, 014524 (2002).
- ³²S. Sanna, G. Allodi, G. Concas, A. D. Hillier, and R. De Renzi, *Phys. Rev. Lett.* **93**, 207001 (2004).
- ³³K. M. Kojima, S. Uchida, Y. Fudamoto, I. M. Gat, M. I. Larkin, Y. J. Uemura, and G. M. Luke, *Physica B* **326**, 316 (2003).
- ³⁴C. Panagopoulos, J. R. Cooper, T. Xiang, Y. S. Wang, and C. W. Chu, *Phys. Rev. B* **61**, R3808 (2000).
- ³⁵S. Kawamata, K. Okuda, T. Sasaki, and R. Yoshizaki, *J. Low Temp. Phys.* **117**, 891 (1999).
- ³⁶K. M. Shen, Ph. D. thesis, Stanford University, 2005.
- ³⁷T. Yoshida, X. J. Zhou, D. H. Lu, S. Komiya, Y. Ando, H. Eisaki, T. Kakeshita, S. Uchida, Z. Hussain, Z.-X. Shen, and A. Fujimori, *J. Phys.: Condens. Matter* **19**, 125209 (2007).
- ³⁸M. Plate, J. D. F. Mottershead, I. S. Elfimov, D. C. Peets, R. Liang, D. A. Bonn, W. N. Hardy, S. Chiuzbaian, M. Falub, M. Shi, L. Patthey, and A. Damascelli, *Phys. Rev. Lett.* **95**, 077001 (2005).
- ³⁹J. K. Perry, J. Tahir-Kheli, and W. A. Goddard III, *Phys. Rev. B* **65**, 144501 (2002).
- ⁴⁰C. T. Chen, L. H. Tjeng, J. Kwo, H. L. Kao, P. Rudolf, F. Sette, and R. M. Fleming, *Phys. Rev. Lett.* **68**, 2543 (1992).
- ⁴¹E. S. Božin and S. J. L. Billinge, *Phys. Rev. B* **72**, 174427 (2005).
- ⁴²R. Khasanov, A. Shengelaya, A. Maisuradze, F. La Mattina, A. Bussmann-Holder, H. Keller, and K. A. Müller, *Phys. Rev. Lett.* **98**, 057007 (2007).
- ⁴³Y. J. Uemura, *Physica C* **282-287**, 194 (1997).
- ⁴⁴W.-G. Yin and W. Ku, arXiv:cond-mat/0702469 (unpublished).